Activation of Src induces mitochondrial localisation of de2-7EGFR (EGFRvIII) in glioma cells: implications for glucose metabolism

Anna N. Cvrljevic[1,2], David Akhavan[3], Min Wu[4], Paul Martinello[5], Frank B. Furnari[6], Amelia J. Johnston[7], Deliang Guo[3], Lisa Pike[4], Webster K. Cavenee[6], Andrew M. Scott[1], Paul S. Mischel[3], Nick J. Hoogenraad[7] and Terrance G. Johns[2,*]

[1]Tumour Targeting Program, Ludwig Institute for Cancer Research, Heidelberg, Victoria 3084, Australia
[2]Oncogenic Signalling Laboratory, Monash Institute of Medical Research, Clayton, Victoria 3168, Australia
[3]Departments of Pathology and Laboratory Medicine and Molecular and Medical Pharmacology and The Jonsson Comprehensive Cancer Center at The David Geffen UCLA School of Medicine, Los Angeles, CA 90095-3075, USA
[4]Seahorse Bioscience, North Billerica, MA 01862-2500, USA
[5]Austin Health, Heidelberg, Victoria 3084, Australia
[6]Ludwig Institute for Cancer Research, San Diego Branch, University of California, San DiegoLa Jolla, CA 92093-0660, USA
[7]Deptartment of Biochemistry, La Trobe University, Bundoora, Victoria 3086, Australia
*Author for correspondence (Terry.Johns@monash.edu)

Accepted 4 May 2011
Journal of Cell Science 124, 2938–2950

doi: 10.1242/jcs.083295

Summary

A common mutation of the epidermal growth factor receptor in glioma is the de2-7EGFR (or EGFRvIII). Glioma cells expressing de2-7EGFR contain an intracellular pool of receptor with high levels of mannose glycosylation, which is consistent with delayed processing. We now show that this delay occurs in the Golgi complex. Low levels of de2-7EGFR were also seen within the mitochondria. Src activation dramatically increased the amount of mitochondrial de2-7EGFR, whereas its pharmacological inhibition caused a significant reduction. Because de2-7EGFR is phosphorylated by Src at Y845, we generated glioma cells expressing a Y845F-modified de2-7EGFR. The de2-7EGFR(845F) mutant failed to show mitochondrial localisation, even when co-expressed with constitutive active Src. Low levels of glucose enhanced mitochondrial localisation of de2-7EGFR, and glioma cells expressing the receptor showed increased survival and proliferation under these conditions. Consistent with this, de2-7EGFR reduced glucose dependency by stimulating mitochondrial oxidative metabolism. Thus, the mitochondrial localisation of de2-7EGFR contributes to its tumorigenicity and might help to explain its resistance to some EGFR-targeted therapeutics.

Key words: EGFRvIII, Mitochondria, Glucose metabolism, Src

Introduction

Glioblastoma multiforme (GBM) is the most common and aggressive form of brain neoplasma affecting adults (Maher et al., 2001). The amplification of the *EGFR* gene is a common event in GBMs and is often accompanied by *EGFR* gene rearrangement (Ekstrand et al., 1992; Sugawa et al., 1990; Wong et al., 1992; Yamazaki et al., 1990); with the most common EGFR mutant found being the de2-7EGFR (or EGFRvIII) (Frederick et al., 2000). This mutant consists of an in-frame deletion spanning exons 2–7 of the coding sequence, resulting in the deletion of 267 amino acid residues from the extracellular domain and the insertion of a novel glycine residue at the junction site (Humphrey et al., 1991; Sugawa et al., 1990). As a result of this truncation, the de2-7EGFR is unable to bind any known ligand. Despite this, de2-7EGFR displays low level constitutive kinase activity that leads to the prolonged activation of downstream signalling pathways (Chakravarti et al., 2004; Li et al., 2004; Moscatello et al., 1998; Narita et al., 2002), partially due to the impaired internalisation and subsequent down-regulation of the receptor (Nishikawa et al., 1994; Schmidt et al., 2003).

Previous studies have demonstrated that the human-derived U87MG glioma cells expressing the de2-7EGFR have an in vivo growth advantage over the wild-type (wt) EGFR (Nishikawa et al., 1994). The enhanced tumorgenicity mediated by de2-7EGFR-expressing cells in part results from direct association or crosstalk between this truncated receptor and other cell-surface receptors such as the wtEGFR and Met (Huang et al., 2007; Luwor et al., 2001; Pillay et al., 2009). Prolonged activation of the PI3K–Akt pathway appears to be a central element of signalling in both GBM tumour samples (Chakravarti et al., 2004), as well as in human-derived GBM cell lines expressing the de2-7EGFR (Li et al., 2004; Moscatello et al., 1998; Narita et al., 2002). Recently, we demonstrated that the de2-7EGFR expressed in U87MG cells is constitutively phosphorylated at tyrosine 845 (Y845) by a member of the Src family kinases (SFKs) (Johns et al., 2007). Given that Y845 has been identified as the site responsible for the activation of Stat3 signalling by the wtEGFR (Mizoguchi et al., 2006), activation of this pathway might also be related to de2-7EGFR tumorgenicity.

There are two reports from the same group showing that wtEGFR can translocate to the mitochondria (Boerner et al.,

2004; Demory et al., 2009). The authors hypothesised a mitochondrial localisation after showing that a phosphorylated, but not unphosphorylated, peptide containing Y845 bound the mitochondrial protein CoxII. They then showed that the wtEGFR could translocate to the mitochondria following ligand stimulation in the presence of Src, where it can phosphorylate CoxII. Mitochondrial localisation of wtEGFR appeared to be important in mediating the EGF protection of breast cancer cells from adriamycin-induced apoptosis. One concern is that this group did not show that their mitochondrial preparations were free of contaminating membranes from other organelles.

Using multiple techniques, we now demonstrate that the de2-7EGFR expressed in human-derived glioma cells is also colocalised with the mitochondria, an observation dramatically enhanced by activation of Src. Using the SFK inhibitor Dasatinib, as well as catalytically impaired Src or Y845 mutants, we demonstrated that the translocation of the de2-7EGFR to the mitochondria is dependent upon the phosphorylation of Y845 by Src. We also demonstrate in this present study, that the de2-7EGFR located at the mitochondria is fully glycosylated and constitutively active, implicating a functionally significant role for this receptor in the mitochondria.

Results

Localisation of de2-7EGFR in human U87MG glioma cells

The detection of ER-associated high-mannose forms of the de2-7EGFR on the plasma membrane (Johns et al., 2005) shows that the normal quality control mechanisms associated with glycoproteins might be overwhelmed by this mutant receptor. Therefore, using confocal microscopy techniques, we examined the localisation of the de2-7EGFR in human U87MG glioma cells. Confocal microscopy images acquired from fixed and permeabilised U87MG.Δ2-7 cells, immunostained with the de2-7EGFR-specific monoclonal antibody (mAb) 806 (Johns et al., 2002), demonstrated colocalisation with cadherins at the plasma membrane (supplementary material Fig. S1A) and the existence of a large intracellular pool of de2-7EGFR (supplementary material Fig. S1A).

De2-7EGFR associates with the ER and Golgi

We then determined whether the intracellular de2-7EGFR in U87MG glioma cells was localised within the ER or Golgi using organelle-specific antibodies. It was difficult to detect the de2-7EGFR in the ER by confocal microscopy (supplementary material Fig. S1B) and subsequent western blotting only detected small amounts of unglycosylated nascent receptor (supplementary material Fig. S2). Thus, only a small component of the intracellular de2-7EGFR is located within the ER. Localisation of the de2-7EGFR to the Golgi complex was examined using mAb 806 and the Golgi antibody ab24586, which specifically binds giantin. Images acquired by confocal microscopy clearly demonstrate the localisation of the de2-7EGFR within the Golgi complex (supplementary material Fig. S1C). These findings suggest that the de2-7EGFR is rapidly transported from the ER to the Golgi, where the process of terminal glycosylation is delayed, resulting in the accumulation of the high-mannose form of de2-7EGFR.

The mitochondrial localisation of de2-7EGFR in U87MG-derived cell lines

The specificity of mAb 806 for de2-7EGFR was confirmed by its lack of staining on U87MG parental cells that express the wtEGFR (supplementary material Fig. S3). The mitochondrial localisation of de2-7EGFR in U87MG.Δ2-7 cells was also assessed, and revealed colocalisation between mAb 806 and MitoTracker Red (MTR) (Fig. 1A). A small amount of de2-7EGFR was located with the mitochondria (Fig. 1A, overlay), as confirmed by voxel analysis of the acquired images (Fig. 1A, image zoom). Given this result, we examined whether the Src-dependent phosphorylation site of Y845 in the de2-7EGFR cells was phosphorylated. Consistent with our previous report (Johns et al., 2007), Y845 was phosphorylated and this phosphorylation was blocked by SFK inhibitors (Fig. 1B), whereas phosphorylation of a major trans-phosphorylation site, Y1173, was unaffected by either SFK inhibitor.

We further investigated this result by determining the expression level of Src in U87MG.Δ2-7 cells. Using intracellular FACS, U87MG.Δ2-7 cells showed low but reproducible levels of Src (Fig. 1C, bottom left). Because the mitochondria localisation of the wtEGFR required overexpression of Src, we generated U87MG.Δ2-7 cells expressing modest levels of activated Src or a dominant-negative form of Src (DNSrc). As expected, transfection of these constructs led to an increase in total Src (Fig. 1C, bottom), but retained similar levels of surface de2-7EGFR as determined by FACS (Fig. 1C, top).

Activated Src increases de2-7EGFR translocation to the mitochondria

We examined the influence of Src activation on the translocation of the de2-7EGFR to the mitochondria. U87MG.Δ2-7_{DNSrc} cells were devoid of mitochondrial localised de2-7EGFR (Fig. 1D, top). By contrast, de2-7EGFR was clearly colocalised with the mitochondria in cells expressing activated Src (Fig. 1D, bottom). Indeed, the general increase in intracellular de2-7EGFR was very evident (Fig. 1D, compare top left panel with bottom left panel). Multiple '*z*-section stack' confocal microscopy images of U87MG.Δ2-7 cell lines (supplementary material Fig. S4) were analysed using ImageJ (NIH). Voxel analysis of these images, showed that significantly more of the total de2-7EGFR expressed in U87MG.Δ2-7_{Src} cells was localised to the mitochondria compared with U87MG.Δ2-7_{DNSrc} cells (24.4% versus 4.1%, respectively; $P<0.0001$) (Fig. 1E). This result suggests that the de2-7EGFR translocates to the mitochondria in a Src-dependent manner.

Analysis of de2-7EGFR in purified mitochondria

To support the confocal microscopy analysis, we purified mitochondria and analysed it for the presence of de2-7EGFR by immunoblotting. Fig. 2A shows the western blot analysis of isolated mitochondria washed multiple times with high-salt buffer. Along with mitochondrial marker Cpn60, this mitochondria fraction contained detectable amounts of lysosomal and ER proteins but was totally devoid of markers for plasma membrane or Golgi (Fig. 2A); the two other organelles contained full-length de2-7EGFR. Additional high-salt washing of the mitochondrial fraction from Fig. 2A resulted in a fraction devoid of mitochondria but enriched in endoplasmic reticulum. This 'Endo' fraction also contained some lysosomal membrane (Fig. 2B). Full-length de2-7EGFR was not detected in this Endo fraction (Fig. 2C), which is consistent with our observation that the ER only contains a small amount of a low molecular mass (100 kDa) nascent form of de2-7EGFR (supplementary material Fig. S2). Furthermore, we have previously demonstrated that

de2-7EGFR in lysosomal compartments is degraded (Perera et al., 2005). Because the mitochondrial-enriched sample only contained full-length de2-7EGFR in a western blot (Fig. 2A, bottom panel) it must be derived from the mitochondria component of the preparation, and not the ER or lysosomal components.

Modulation of the mitochondrial translocation of the de2-7EGFR by Dasatinib

Having demonstrated that Src activation is required for de2-7EGFR localisation to the mitochondria, we sought to confirm the importance of Src kinase activity in modulating mitochondrial translocation. To address this question, mitochondria were

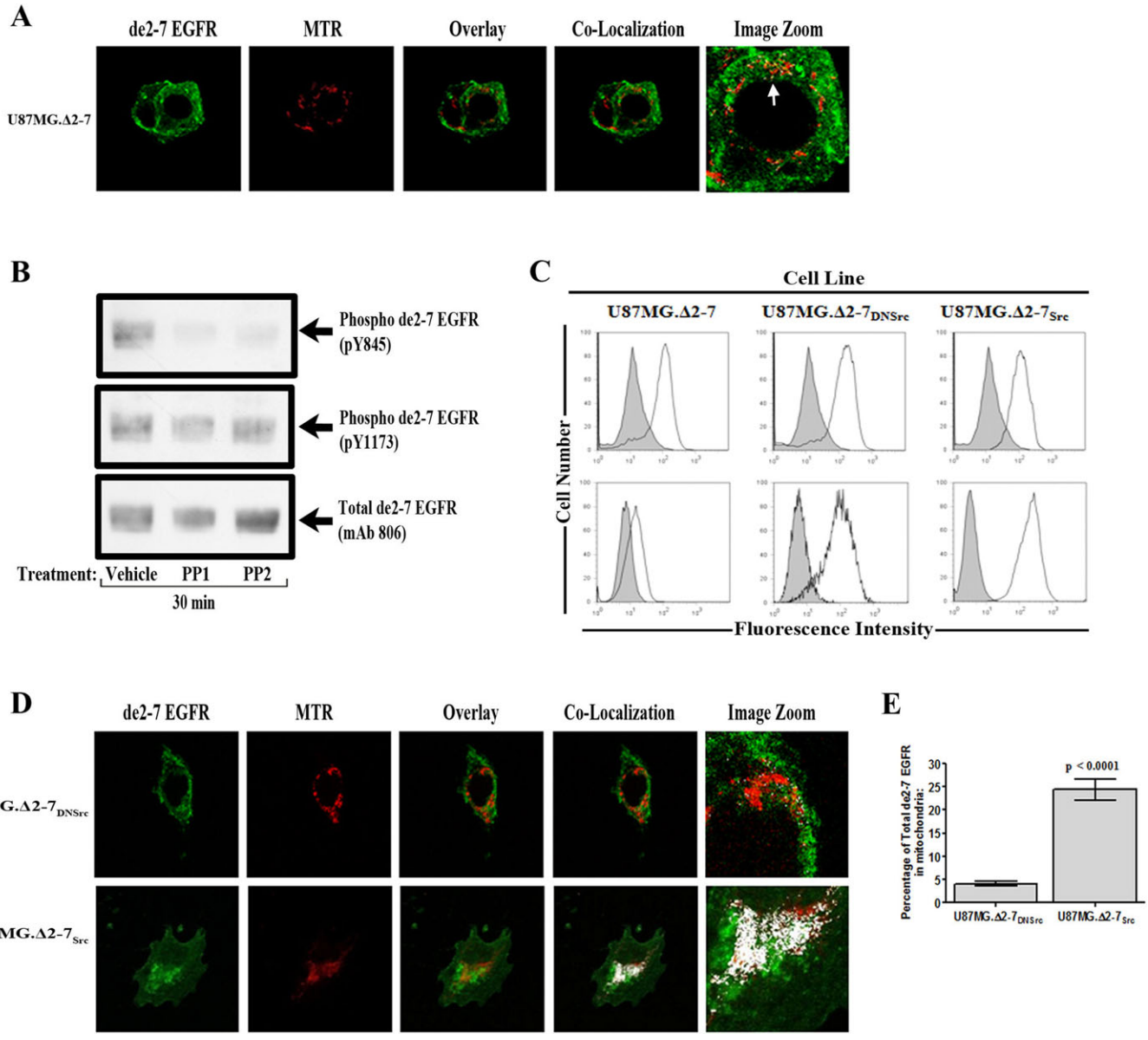

Fig. 1. The mitochondrial localisation of the de2-7EGFR in U87MG-derived cell lines. (**A**) Low levels of de2-7EGFR colocalise with the mitochondria (arrow) in U87MG.Δ2-7 cells immunostained with mAb806 and MTR. (**B**) Lysates from U87MG.Δ2-7 cells treated with SFK inhibitors, PP1 or PP2 (10 μM) were immunoprecipitated with the pan-EGFR antibody mAb528. Inhibition of SFKs, blocked phosphorylation of de2-7EGFR at the Src-dependent phosphorylation site Y845 (top), but had no effect on phosphorylation of de2-7EGFR at a major auto-phosphorylation site, Y1173 (middle). Total de2-7EGFR levels were confirmed using mAb 806 (bottom). (**C**) Similar levels of surface de2-7EGFR expression were observed in three different U87MG.Δ2-7 derived cell lines (top panel, open histogram) as measured by FACS. The level of intracellular Src in the different U87MG.Δ2-7 cell lines was determined by intracellular FACS using a Src specific antibody (bottom panel, open histogram). Shaded histograms represent negative-control antibodies. (**D**) Voxel analysis of confocal microscopy images obtained from U87MG.Δ2-7 cells expressing a DNSrc or a constitutive active Src demonstrate that the de2-7EGFR is translocated to the mitochondria in a Src-dependent manner. Green, de2-7EGFR (mAb 806); red, mitochondria (MTR); white, colocalisation. (**E**) Computational analysis of all acquired confocal microscopy images represented in D. Data are expressed as a percentage of total de2-7EGFR expressed by the cell found colocalised with mitochondria.

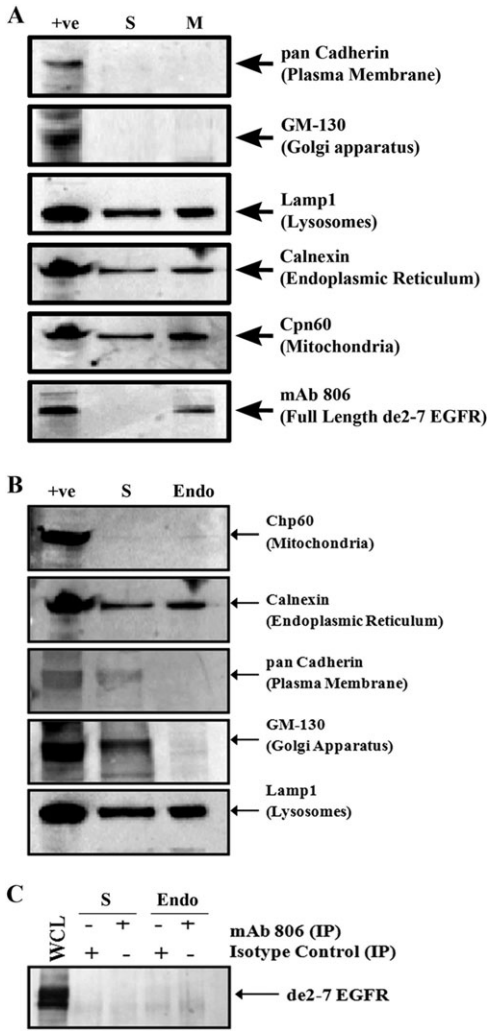

Fig. 2. Analysis of purified mitochondria. (**A**) Enriched mitochondria (M), isolated from U87MG.Δ2-7$_{Src}$ cells were assessed by immunoblotting for purity against the following panel of organelle marker antibodies: plasma membrane (pan cadherin, 1:100); Golgi (GM-130, 1:1000); lysosomes (LAMP1, 1:1000); ER (anti-calnexin, 1:5000) and mitochondria (Cpn60, 1:10,000). A whole-cell lysate (WCL) sample served as a control (+ve). Supernatant (S) represents the cellular components and debris removed from mitochondria following the final high-salt wash. Localisation of the de2-7EGFR within the mitochondria fraction was confirmed using mAb806 (bottom panel). (**B**) The mitochondrial fraction from A was purified further to obtain a membrane fraction (Endo) enriched in ER and lysosomes. (**C**) The membrane Endo fraction from B was probed for expression of de2-7EGFR; full length de2-7EGFR was clearly absent from this preparation.

isolated from U87MG.Δ2-7$_{Src}$ cells treated with either the SFK inhibitor Dasatinib (150 ng/ml) or vehicle, under serum-free conditions. This dose of Dasatinib is sufficient to inhibit the constitutive active Src expressed in these cells (Lu et al., 2009). Purified mitochondria were resolved by SDS-PAGE with equal loading confirmed by immunoblotting for the mitochondrial marker antibody, Cpn60 (Fig. 3A, bottom panel). Immunoblot analysis of the samples using mAb 806, which under denaturing conditions acts as a pan-EGFR antibody (Fig. 3A, top panel), demonstrated that both the de2-7EGFR and wtEGFR are localised within the mitochondria of U87MG.Δ2-7$_{Src}$ control cells. Dasatinib completely ablated localisation of wtEGFR within mitochondria and caused a marked reduction in the level of de2-7EGFR localised within the mitochondria (Fig. 3A, top panel). Quantification of four independent experiments demonstrated a significant 33% reduction in de2-7EGFR localisation within the mitochondria in cells treated with Dasatinib relative to vehicle control ($P=0.002$; Fig. 3B, left panel). Because the half-life of de2-7EGFR in mitochondria is unknown, it is possible that the remaining receptor observed after 24 hours of Dasatinib treatment is part of the pre-existing pool within the mitochondria.

Immunoblot analysis using an anti-EGFR antibody that specifically recognises phosphorylation of Y845 confirmed that the de2-7EGFR localised within the mitochondria is phosphorylated at this Src phosphorylation site (Fig. 3A, second panel). As expected, Dasatinib led to a significant reduction in the level of Y845-phosphorylated de2-7EGFR within the mitochondria ($P=0.01$; Fig. 3B, middle panel). Phosphorylation at a major auto-phosphorylation site of the de2-7EGFR (Y1173) was also seen in receptor isolated from mitochondria (Fig. 3A, third panel), further confirming that mitochondrial-located de2-7EGFR is active and potentially capable of signalling within this organelle. However, unlike results for phosphorylation at Y845, the amount of de2-7EGFR phosphorylated at Y1173 was not significantly lower in cells treated with Dasatinib ($P>0.05$) (Fig. 3B, right panel).

The influence of Dasatinib on de2-7EGFR localisation to the mitochondria was further examined by confocal microscopy. Voxel analysis of acquired confocal microscopy images demonstrated a significant reduction in the level of de2-7EGFR colocalised with the mitochondria (Fig. 3C, image zoom). Computational analysis of cells revealed varying levels of de2-7EGFR colocalised in the mitochondria, which is consistent with the heterogeneity of cell lines used (Fig. 3D, left panel). However, quantification of cells examined clearly showed a significant reduction in de2-7EGFR in the mitochondria following Dasatinib treatment (Fig. 3D, right panel; $P=0.002$). Indeed, the 33% was virtually identical to that obtained by immunoblotting analysis (cf. Fig. 3B, left panel).

Mitochondrial localisation of de2-7EGFR following activation of Src by ECM proteins

Having demonstrated that Src activity modulates the translocation of de2-7EGFR to the mitochondria, we wanted to confirm this result in a system that is not reliant on transfected Src. Thus, U87MG.Δ2-7 cells were grown on uncoated coverslips or coverslips covered with a thin layer of matrigel and then examined by confocal microscopy. Matrigel contains a number of ECM proteins known to activate Src and other molecules through engagement with integrins (Clark and Brugge, 1995). A significant increase in mitochondrial de2-7EGFR was demonstrated following plating of U87MG.Δ2-7 cells on matrigel (Fig. 4A, bottom panel). Voxel analysis of cells revealed that virtually all cells grown on matrigel and all mitochondria in these cells contained de2-7EGFR (Fig. 4B). Quantitative analysis showed that the amount of mitochondria colocalised with de2-7EGFR following engagement with matrigel increased from 33% to 99% ($P<0.0001$; Fig. 4B). To test whether the ECM component of Matrigel could mediate phosphorylation of the Y845 residue, U87MG.Δ2-7 cells were plated on uncoated plastic or plastic coated with collagen, which makes up 30% of the Matrigel ECM. Collagen stimulated a robust phosphorylation of de2-7EGFR at multiple tyrosine sites including Y845, when compared with results on plastic (supplementary material Fig. S5).

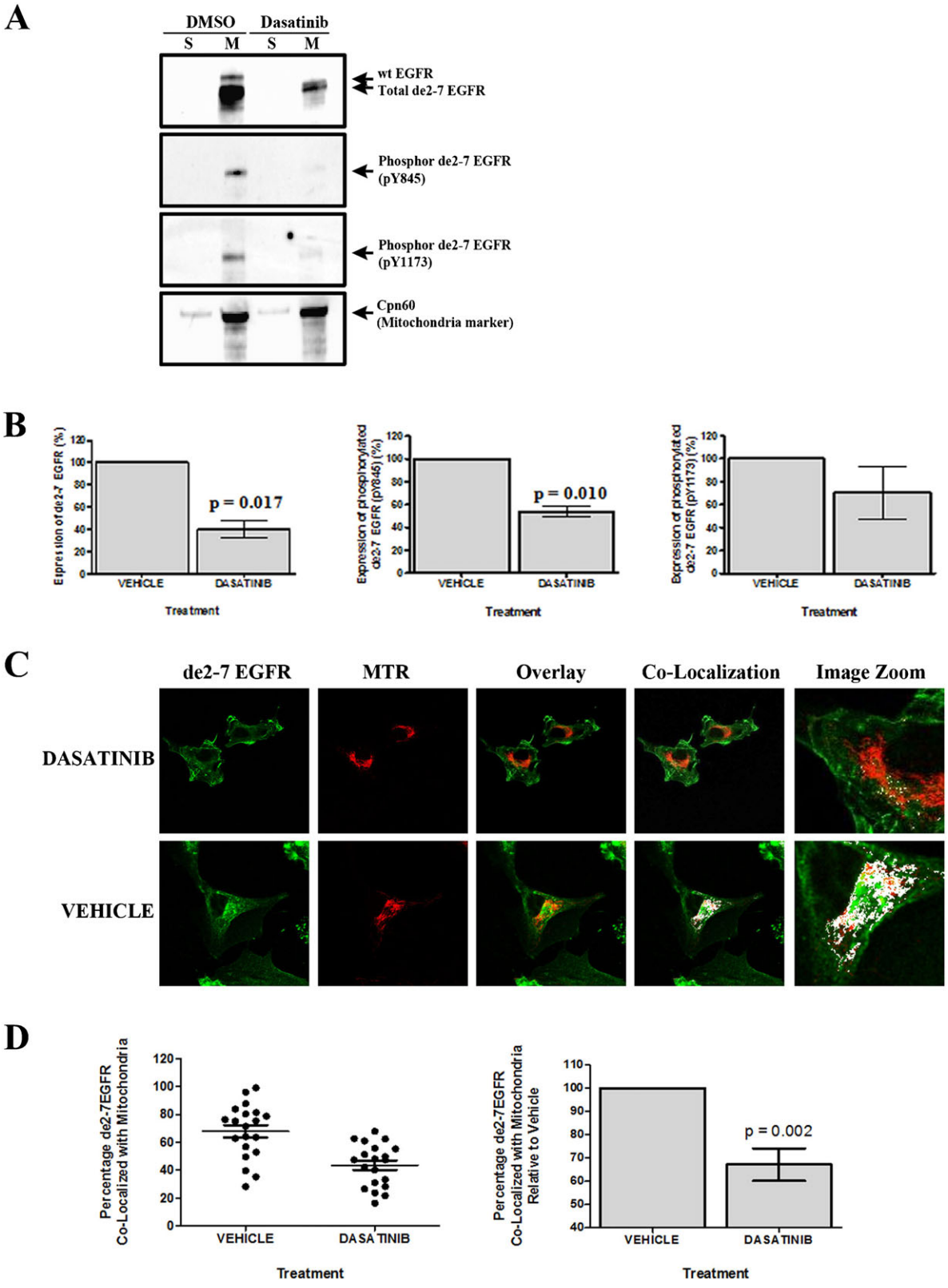

Fig. 3. See next page for legend.

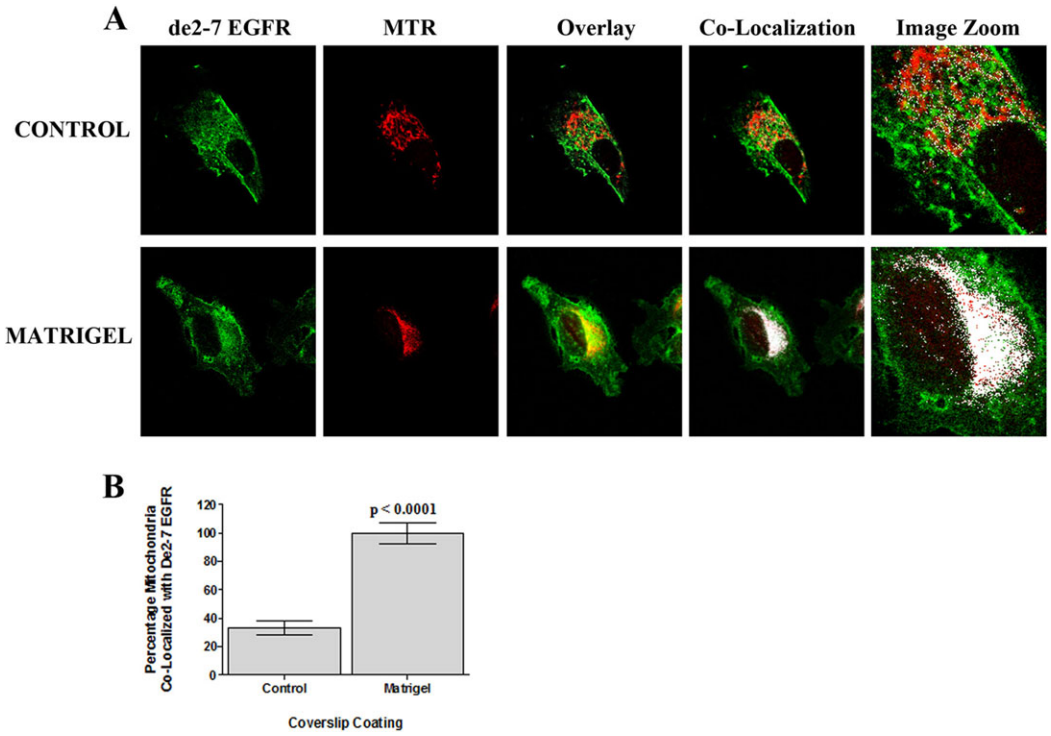

Fig. 4. Matrigel activation of the de2-7EGFR induces mitochondrial translocation. U87MG.Δ2-7 cells grown on a thin layer of Matrigel or on uncoated coverslips (control) were assessed for mitochondrial localisation of the de2-7EGFR by confocal microscopy. (**A**) Green, de2-7EGFR (mAb806); red, mitochondria (MTR); white, colocalisation. (**B**) Histogram quantifying the mean increase in mitochondrial associated de2-7EGFR following attachment to Matrigel. Data are expressed as mean percentage ± s.e. (n=233).

Interestingly, collagen stimulated Y845 phosphorylation above the level of de2-7EGFR from cells grown in serum.

The translocation of the de2-7EGFR to the mitochondria is dependent on phosphorylation of Y845

All our evidence suggests that the phosphorylation of Y845 by Src is required for de2-7EGFR mitochondrial localisation. Therefore we constructed a cell line co-expressing de2-7EGFR with a Y845F modification (i.e. unable to be phosphorylated by Src) and activated Src. FACS analysis confirmed that the level of de2-7EGFR expressed on the surface of U87MG.Δ2-7_{845F} cells was not compromised following the transfection of cells to produce the U87MG.Δ2-$7_{845F.Src}$ cell line (Fig. 5A, top panel). Intracellular FACS analysis clearly demonstrates the increase in Src expression following transfection with activated Src (Fig. 5A, bottom panel).

Analysis of U87MG.Δ2-7_{845F} cells by confocal microscopy clearly demonstrates the lack of de2-7EGFR colocalised with the mitochondria (Fig. 5B, top panel). More importantly, expression of activated Src in the U87MG.Δ2-7_{845F} cells failed to induce the mitochondrial localisation of de2-7EGFR Y845F (Fig. 5B, middle panel). As previously, the U87MG.Δ2-7_{Src} cells showed clear localisation of de2-7EGFR in the mitochondria (Fig. 5B, bottom panel). These results demonstrate that the activation of Y845 by Src is essential for the translocation of the receptor to the mitochondria and is not merely the result of increased Src activity.

Localisation of the de2-7EGFR within the mitochondria

Having demonstrated that de2-7EGFR colocalises with the mitochondria, we examined the outer membrane of intact mitochondria isolated from U87MG and U87MG.Δ2-7_{Src} cells for de2-7EGFR localisation by electron microscopy (EM). De2-7EGFR on the outer membrane surface of mitochondria was visualised using mAb 806 and a gold-labelled anti-mouse secondary antibody. The mitochondria from U87MG.Δ2-7_{Src} cells (Fig. 6A), but not from U87MG parental cells, were positive

Fig. 3. Dasatinib modulates the mitochondrial translocation of the de2-7EGFR. U87MG.Δ2-7_{Src} cells were incubated with the SFK inhibitor, Dasatinib (150 ng/ml) or vehicle control (0.01%, DMSO) under serum-free conditions for 24 hours. (**A**) Purified mitochondria (M) and supernatant (S) samples were analysed by immunoblot using de2-7EGFR specific (mAb 806; top) or phospho-EGFR-specific antibodies (EGFR-pY845; 1:250 or EGFR-pY1173; 1:500; middle panels). Equal loading was confirmed using the mitochondrial marker Cpn60 (bottom). (**B**) Densitometric analysis of western blots in A was performed by measuring differences in total and phosphorylated de2-7EGFR within the mitochondria of treated or untreated cells normalised to Cpn60. Values depict results from four independent experiments, expressed here as mean percentage ± s.e. relative to vehicle. (**C**) The effect of inhibiting SFKs with Dasatinib (top) compared with vehicle (bottom) on the translocation of de2-7EGFR to the mitochondria in U87MG.Δ2-7_{Src} cells as assessed by confocal microscopy. Green, de2-7EGFR (mAb806); red, mitochondria (MTR); white, colocalisation. (**D**) Scatter plots prepared using a subset of cells to demonstrate the range of localisation seen in the vehicle and dasatinib groups. Points representing the percentage of mitochondria associated with de2-7EGFR within individual cells are shown, along with the mean ± s.e. (left panel). Histogram showing the quantifying the mean decrease in mitochondrial associated de2-7EGFR following Dasatinib treatment (n=133). Data are expressed as mean percentage ± s.e. (right).

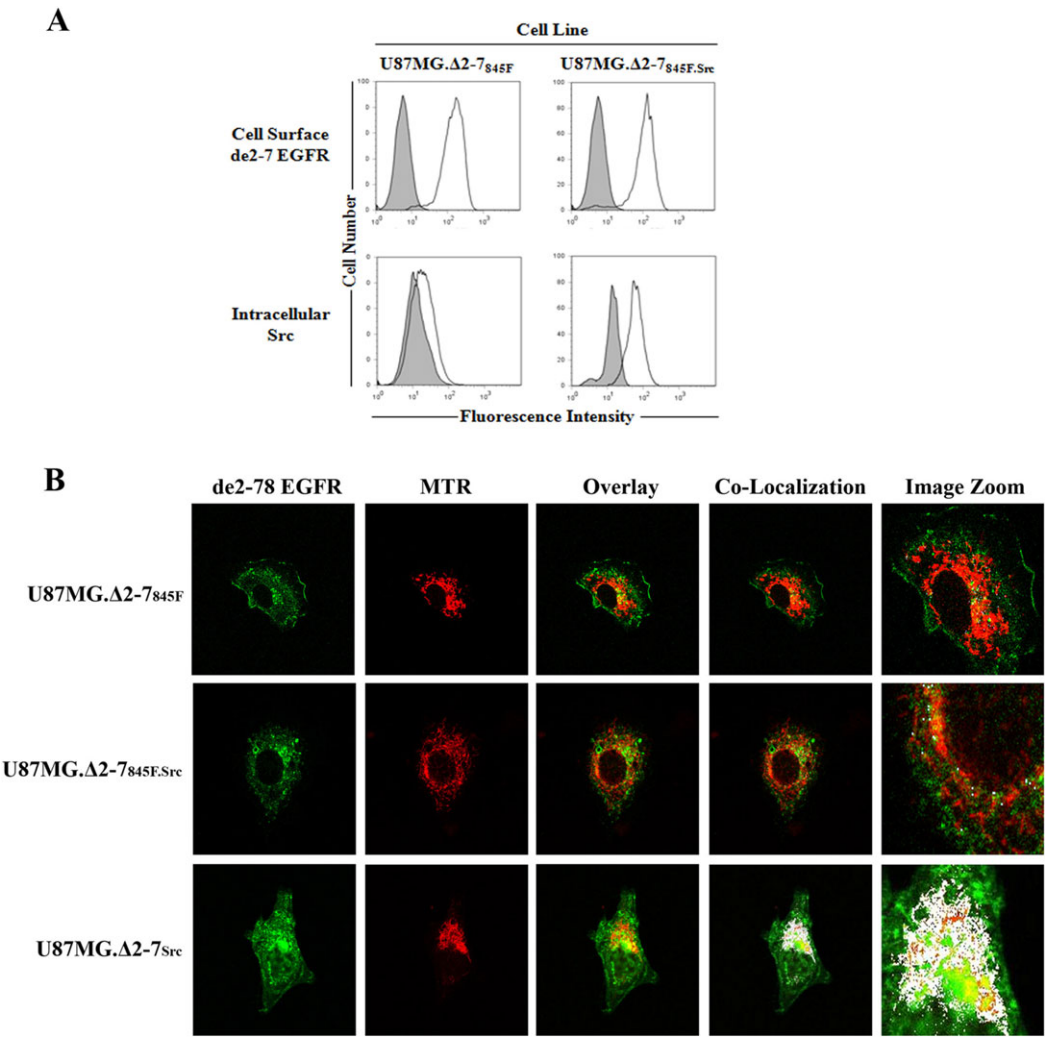

Fig. 5. The mitochondrial translocation of the de2-7EGFR is dependent upon Y845 phosphorylation. (**A**) The cell surface expression of the de2-7EGFR with a Y845F mutation expressed in U87MG cells was assessed by FACS (top panel) using an irrelevant antibody (shaded histogram) or the de2-7EGFR- specific antibody mAb806 (open histogram). The expression of activated Src following transfection into U87MG.Δ2-7_{845F} cells was assessed by intracellular FACS using a Src specific antibody (open histogram) or irrelevant control antibody (shaded histogram). (**B**) Mitochondrial localisation of the Y845F modified de2-7EGFR in the absence (top panel) or presence (middle panel) of activated Src was assessed by confocal microscopy. The U87MG.Δ2-7_{Src} cell line was used as a positive control for mitochondrial localisation of de2-7EGFR. Computational analysis of colocalisation was performed using ImageJ. Green, de2-7EGFR (mAb 806); red, mitochondria (MTR); white, colocalisation.

for surface de2-7EGFR. Of a total of 126 mitochondria from U87MG.Δ2-7_{Src} cells analysed by EM, 76% were positive for de2-7EGFR, compared with 0% of 82 mitochondria from U87MG cells (Chi square=77.94, d.f.=1, $P<0.0001$). This result confirms the presence of de2-7EGFR in the mitochondria by a third independent technique, and suggests that the de2-7EGFR is localised in the outer mitochondrial membrane, although the orientation of the receptor is not known.

We treated purified mitochondria isolated from U87MG.Δ2-7_{Src} cells with proteinase K (PK) (Gough et al., 2009; Vande Velde et al., 2008). The level of de2-7EGFR detected in the mitochondria was significantly reduced in samples treated with PK compared with sham-treated samples (Fig. 6B, top panel). Thus, consistent with the EM data, this demonstrates that some of the de2-7EGFR is located on the surface of mitochondria and accessible to PK. However, the presence of some PK-resistant de2-7EGFR suggests that some of the de2-7EGFR is located within the mitochondria (Fig. 6B, top panel).

Limiting the supply of glucose increases mitochondrial de2-7EGFR

Given that de2-7EGFR preferentially activates the PI3-K–Akt pathway in glioma cell lines and tumour samples (Chakravarti et al., 2004; Li et al., 2004; Moscatello et al., 1998; Narita et al., 2002), which in turn increases cellular metabolism by increased aerobic glycolysis and lipogenesis (Guo et al., 2009; Swinnen et al., 2006; Warburg, 1956b), we examined the effect of low glucose on de2-7EGFR localisation. There was an increase in de2-7EGFR colocalised with the mitochondria following a reduction of glucose in the cell medium (Fig. 7A). A detailed statistical analysis showed that the proportion of mitochondria containing de2-7EGFR was significantly higher in the 1.6 g/l

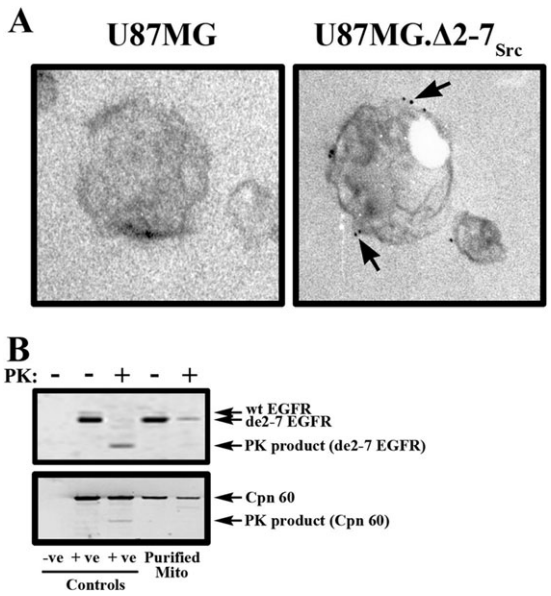

Fig. 6. Localisation of de2-7EGFR with mitochondria. (**A**) The outer membrane surface of mitochondria isolated from the U87MG parental cells, which lack de2-7EGFR expression (negative control), or U87MG.Δ2-7_{Src} cells were analysed by EM for de2-7EGFR, using mAb806 counterstained with gold-labelled anti-mouse (arrow, de2-7EGFR). (**B**) Susceptibility of de2-7EGFR in enriched mitochondria from U87MG.Δ2-7_{Src} cells to protease digestion was examined by western blot following treatment with proteinase K (PK). The de2-7EGFR-specific antibody, mAb806, was used to detect de2-7EGFR (top panel), whereas the mitochondrial matrix protein, chaperonin 60 (Cpn60), which given its locality is resistant to PK, was detected using anti-Cpn60 (bottom panel). Controls of whole-cell lysates prepared from U87MG.Δ2-7_{Src} cells were immunoprecipitated with an irrelevant antibody IgG_{2b} to provide a negative control (–ve/–PK) or with mAb806 to provide a positive control for de2-7EGFR (+ve/–PK). Enriched mitochondria lysed with RIPA buffer was incubated with PK at 37℃ for 15 minutes to confirm proteinase PK activity (+ve/+PK).

cohort compared with cells in medium containing 4.5 g/l of glucose (Fig. 7B).

The translocation of de2-7EGFR to the mitochondria under low-glucose conditions suggests that this receptor has a function in protecting glucose-stressed glioma cells. Therefore, we examined the proliferation and viability of U87MG and U87MG.Δ2-7 glioma cell lines in different concentrations of glucose. Both U87MG and U87MG.Δ2-7 cells proliferated in medium containing 25 mM glucose (Fig. 8A,B). Reduction to 5 mM glucose had no effect on U87MG.Δ2-7 cells until day 4, when there was a small decrease in proliferation (Fig. 8B). By contrast, U87MG cells displayed significantly reduced proliferation in 5 mM glucose on all days (Fig. 8A). Neither cell line proliferated at concentrations of glucose less than 1 mM (Fig. 8A,B). U87MG cells were viable in 25 and 5 mM glucose but had low viability in concentrations of 1 mM and less (Fig. 8C). By contrast, U87MG.Δ2-7 cells remained viable at concentrations as low as 0.5 mM glucose, with a significant drop in viability only seen in the complete absence of glucose (Fig. 8D). Thus U87MG.Δ2-7 cells show increased proliferation and survival under glucose stress. U87MG cell lines are null for PTEN, which is a crucial endogenous inhibitor of PI3K. Restoration of PTEN in U87MG.Δ2-7 cells completely re-established the glucose-sensitivity phenotype (supplementary material Fig. S6), highlighting the central role of PI3K in this process. Overall, these results suggest that de2-7EGFR in the mitochondria has a role in regulating glucose metabolism.

Measurement of cellular oxygen consumption rate and extracellular acidification rate

As shown in Fig. 9A, transfection of de2-7EGFR in to U87MG cells increased basal mitochondrial OCR but decreased extracellular acidification rate ECAR or glycolysis rate (i.e. the U87MG.Δ2-7 cells moved to a more oxidative metabolic phenotype). Given this observation, we explored whether de2-7EGFR alters mitochondrial function. Mitochondrial function was assessed by the sequential addition of oligomycin (ATP synthase inhibitor), FCCP (uncoupler of oxidative phosphorylation) and antimycin (complex III inhibitor) to cells; thus allowing determination of the ATP-coupled respiration, leaked respiration (proton leak) and maximal respiration capacity. These compounds were titrated for their optimal concentrations in separate experiments. As shown in Fig. 9B, maximal mitochondrial respiration capacity (i.e. FCCP-stimulated OCR) was significantly higher in U87MG.Δ2-7 cells than in U87MG cells. This suggests that the electron transport chain activity is unregulated by de2-7EGFR. Hence, de2-7EGFR not only elevated basal oxygen consumption rate, but also increased mitochondrial bioenergetic function, either through an increase in the number of mitochondria or raised levels of enzymes of the electron transport complex.

Discussion

When expressed in a variety of cell lines de2-7EGFR runs as two distinct bands on SDS-PAGE (Johns et al., 2005). These two bands have also been observed in patient samples (Mellinghoff et al., 2005). Previously, we demonstrated that the lower molecular mass form of the de2-7EGFR corresponds to an immature, high-mannose form of the receptor (Johns et al., 2005). Most of this receptor is found inside the cell, although a small amount was misdirected to the cell surface. The studies described here show that this form of the receptor is concentrated in the Golgi, presumably awaiting terminal glycosylation, not in the ER as might be expected. Because this high-mannose form of the de2-7EGFR is constitutively active, this pool of the receptor might contribute to its tumorigenicity. The observation that signalling molecules downstream of de2-7EGFR, such as Ras, are present and active in the Golgi supports this possibility (Chiu et al., 2002).

Members of the ErbB family are generally anti-apoptotic, and signalling downstream from these receptors can modulate the activity of mitochondria-associated proteins, including the Bcl-2 family (Goel et al., 2007). Recently, it was demonstrated that the transforming activity of ErbB2 could be reduced by overexpressing DecR1 (Ursini-Siegel et al., 2007); a mitochondrial enzyme intimately involved in fatty acid β-oxidation. More surprising are the recent observations that a cleaved intracellular fragment derived from ErbB4 and the full-length wtEGFR can translocate to the mitochondria (Boerner et al., 2004; Naresh et al., 2006). The function of EGFR and ErbB4 located in the mitochondria remains unknown, although a role for EGFR in anti-apoptosis was indicated by its potential interaction with CoxII. Collectively, these studies show a growing relationship between several aspects of mitochondria function and activation of ErbB family members.

Our data definitively show that the cancer-specific de2-7EGFR can also translocate to the mitochondria. This translocation

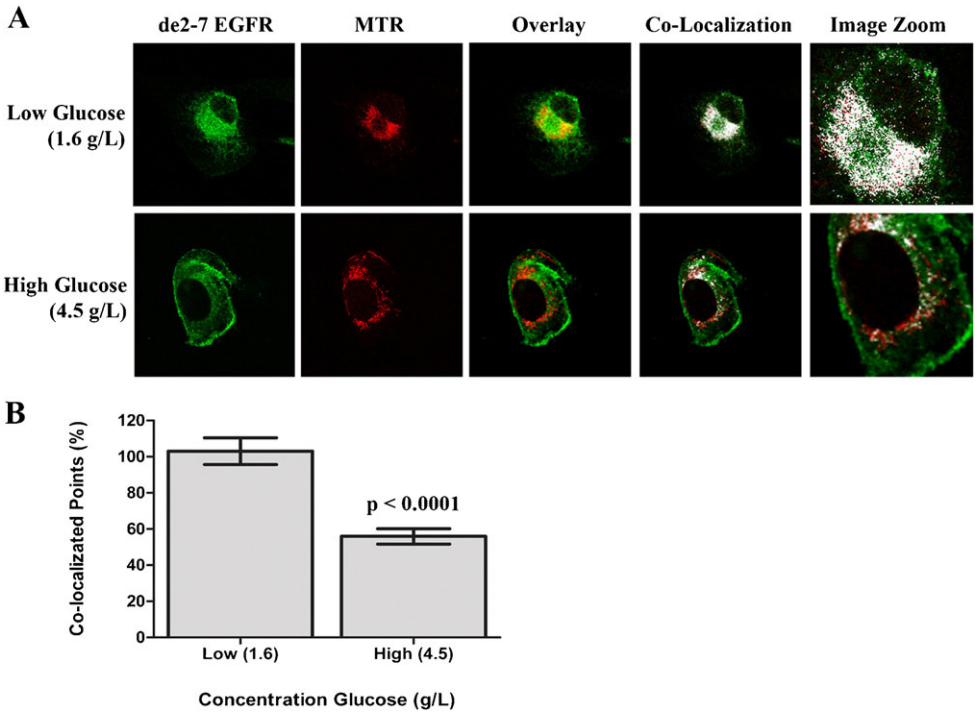

Fig. 7. Low glucose stimulates mitochondrial localisation of the de2-7EGFR. (**A**) The mitochondrial localisation of de-2-7EGFR in U87MG.Δ2-7$_{Src}$ cells grown in low glucose (top panel) or high glucose (lower panel) medium as assessed by confocal microscopy. Green, de2-7EGFR (mAb806); red, mitochondria (MTR); white, colocalisation. (**B**) Histogram quantifying the mean increase in mitochondria-associated de2-7EGFR following the addition of low-glucose medium. Data are expressed as mean percentage ± s.e.

required activation of Src, but not necessarily the overexpression of Src. Unlike the published data for the wtEGFR (Boerner et al., 2004), mitochondrial localisation of de2-7EGFR was entirely dependent on the phosphorylation of Y845 because mutation of this site completely abrogated mitochondrial localisation, even in the presence of constitutively active Src. Because the mitochondrially localised de2-7EGFR was fully glycosylated, it was not derived from the high-mannose pool of intracellular receptor that resides in the Golgi. There is a precedent for these proteins moving from the plasma membrane to other cellular compartments. Both the wtEGFR and de2-7EGFR can traffic to the nucleus (Carpenter and Liao, 2009; de la Iglesia et al., 2008). In the case of the wtEGFR this involves retrograde transport of the receptor from the cell surface by endosomes to the ER. In the ER, the wtEGFR is extracted from the lipid bilayer by interacting with Sec61. Further interaction with chaperones, such as heat shock protein 70 (HSP70), promote the extrusion of wtEGFR into the cytoplasm, where it associates with importin-β, which leads to nuclear import (Carpenter and Liao, 2009). Given that mitochondrial de2-7EGFR is fully glycosylated, we propose that mitochondrial localisation of both the de2-7 and wtEGFR is mediated by a similar process, except once in the cytoplasm, it is

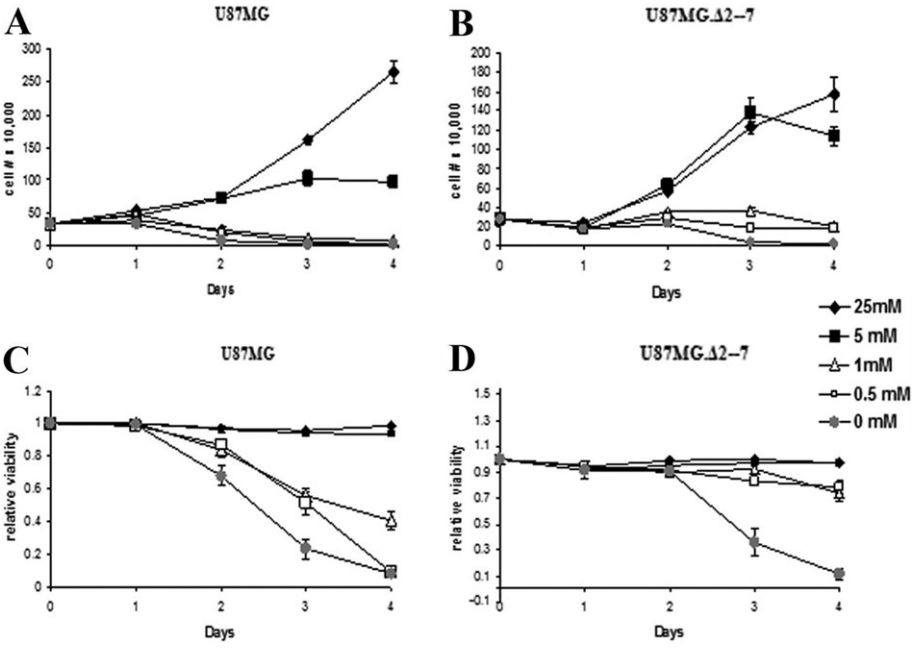

Fig. 8. Growth and viability of U87MG and U87MG.Δ2-7 cells in different concentrations of glucose. U87MG and U87MG.Δ2-7 were grown at the different concentrations of glucose indicated. Cell number (**A**,**B**) and cell viability (**C**,**D**) were then determined daily. Representative experiment is shown and data expressed as the average of four counts ± s.e.

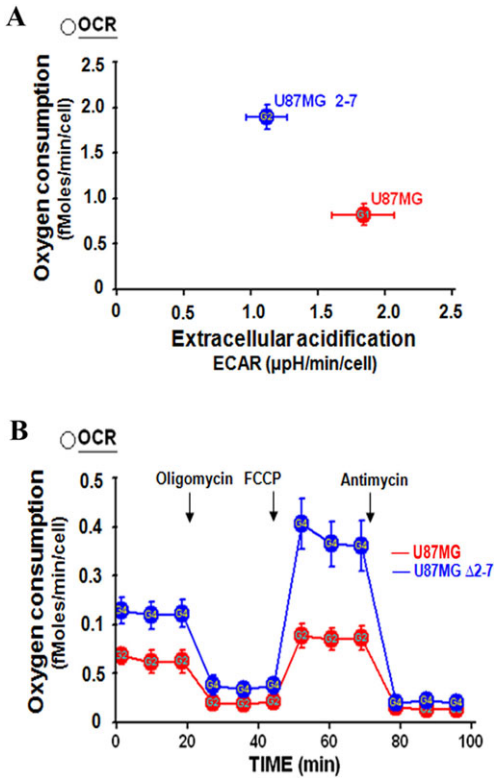

Fig. 9. Measurement of cellular oxygen consumption rate OCR and ECAR. (**A**) Basal OCR and ECAR of the U87MG and U87MG Δ2-7 were measured in assay medium containing 25 mM glucose, 4 mM glutamine and 1 mM pyruvate. (**B**) Cells were switched to assay medium containing 25 mM glucose, 4 mM glutamine and 2 mM pyruvate to determine their mitochondrial function. After baseline measurement, oligomycin, FCCP (0.5 μM) and antimycin (1 μM) were added to the cells to a final concentration of 0.5 μM, 0.125 μM and 1 μM.

directed to the mitochondria. Our results suggest that phosphorylation of the Y845 site in the de2-7EGFR is crucial in the decision to direct it to the mitochondria. Direct confirmation that the sec61 pathway is responsible for de2-7EGFR transport to the mitochondria is the subject of ongoing studies.

De2-7EGFR signalling in glioma cells protects them from apoptosis by increasing expression of Bcl-X_L and therefore does not require the physical presence of the receptor in the mitochondria (Nagane et al., 1998). The wtEGFR was reported to interact with CoxII in the mitochondria by binding to Y845 (Boerner et al., 2004); however, we could not detect a direct interaction of de2-7EGFR with COXII, even though it is constitutively activated at Y845 (data not shown). Recently, it has been reported that de2-7EGFR enhances lipogenesis in U87MG glioma cells (Guo et al., 2009), firmly establishing a role for this receptor in cell metabolism. The above report, and our observations that de2-7EGFR shows increased mitochondrial localisation under low-glucose conditions, indicates that it has a role in modulating cell metabolism. Indeed, the ability of de2-7EGFR to shift U87MG cells towards mitochondrial oxidative metabolism at the expense of aerobic glycolysis, strongly supports a function for this receptor in cell metabolism. Furthermore, this de2-7EGFR-mediated change in cell metabolism should make U87MG.Δ2-7 cells less dependant on glucose; an outcome that is entirely consistent with the enhanced cell survival of U87MG.Δ2-7 cells grown in low-glucose conditions. Given the convergence between metabolic and apoptotic pathways (Bonnet et al., 2007), a central role for de2-7EGFR in metabolic processes related to apoptosis is an attractive hypothesis that we are exploring.

De2-7EGFR is resistant to several EGFR-targeted therapeutics (Fukai et al., 2008; Heimberger et al., 2002; Montgomery, 2002) and other therapeutics show only modest activity (Johns et al., 2007). Our observation that there are two intracellular pools of activated de2-7EGFR (Golgi and mitochondria), provides a possible mechanism for this resistance. Clearly EGFR-specific antibodies would not effectively target these intracellular pools of de2-7EGFR. Given that some of the de2-7EGFR appears to be found in the internal mitochondrial compartments, it is also likely that some small molecules might not effectively inhibit this pool of receptor. Designing EGFR inhibitors that can penetrate the mitochondria membranes might have greater efficacy against this receptor. We have shown that the anti-tumour activity of a de2-7EGFR-specific antibody (mAb806) against U87MG.Δ2-7 glioma xenografts is significantly enhanced if Src activity is inhibited genetically (Johns et al., 2007) or pharmacologically, using dasatinib (Lu et al., 2009). This was achieved using doses of dasatinib that had no therapeutic effect as a sole agent. Our current studies showing that dasatinib prevents the translocation of de2-7EGFR provides an explanation for this increased anti-tumour activity; when there is no intracellular pool of de2-7EGFR, mAb806 can effectively block signalling at the cell surface.

The observation that most cancer cells rely on aerobic glycosylation rather than oxidative phosphorylation (the Warburg effect) (Warburg, 1956a) has long demonstrated an association between the mitochondria and cancer beyond its obvious role in apoptosis. The metabolic requirements and associated role of mitochondria in cancer cells is a topic of increasing interest (Vander Heiden et al., 2009), with one recent paper showing that the pharmacological reversal of the Warburg effect induces cell death in a range of cancer cell lines (Bonnet et al., 2007). As noted above, there is growing evidence that ErbB family members have a role in cell metabolism and mitochondria function. Our work showing significant targeting of the de2-7EGFR to the mitochondria strongly implicates a more direct role for some members of this family in mitochondrial activity.

Materials and Methods

Antibodies and chemical reagents

mAb806, which preferentially recognises de2-7EGFR in U87MG glioblastoma cells and the irrelevant isotype-matched IgG_{2b} antibody (clone 100-310), have been described in detail previously (Johns et al., 2002; Luwor et al., 2001). Both antibodies were produced in the Biological Development Facility (BDF; Ludwig Institute for Cancer Research Ltd, Melbourne). Serum from rabbits immunised with the mitochondrial protein Chaperone-60 (Cpn60), was used as a mitochondrial marker. Antibodies raised against the following antigens were used: giantin (ab24586), pan cadherin (ab6529) (Abcam, Cambridge, MA); calnexin (C-terminal 575–594); v-Src 327 (Ab-1) (Calbiochem, Gibbstown, NJ); Golgi matrix protein 130 (GM-130), lysosome-associated membrane protein 1 (LAMP-1) (BD Transduction Laboratories, Franklin Lakes, NJ); MitoTracker Red (MTR), secondary antibodies: mouse Alexa Fluor 488 and rabbit Alexa Fluor 594 IgG (Molecular Probes, Grand Island, NY); EGFR-pY845, Src-pY418 and EGFR-pY1173 (Biosource International, Cell Signaling Laboratories, Danvers, MA); HRP-conjugated secondary antibody raised against goat IgG (1:10,000), pan phospho-EGFR, pY20 (Santa Cruz Biotechnology, La Jolla, CA); gold-conjugated secondary antibody raised against mouse IgG (1:500) (Sigma, St Louis, MO). HRP-conjugated secondary antibodies raised against mouse (1:10,000) and rabbit (1:2000) IgG were purchased from Chemicon Australia (Millipore, North Ryde, NSW, Australia).

Cell lines

The human derived glioblastoma cell lines U87MG, U87MG.Δ2-7 and U87MG.Δ2-7_{DNSrc} have been described previously (Johns et al., 2007; Nagane et al., 1996; Nishikawa et al., 1994) All cell lines were routinely maintained in DMEM/F-12 (Life Technologies) supplemented with 5% FCS (CSL), 2 mM Glutamax (Sigma) and 2 mM penicillin-streptomycin (Life Technologies). In addition, the transfected U87MG.Δ2-7 cell line was maintained in, 400 μg/ml Geneticin (Life Technologies), whereas the U87MG.Δ2-7_{DNSrc} cell line was maintained in both Geneticin and 100 μg/ml hygromycin (Roche Diagnostics, Mannheim, Germany).

Transfection of cell lines

A mutant form of the de2-7EGFR containing a Y845F substitution was obtained by site-directed mutagenesis. The mutant receptor (Δ2-7_{845F}) was subsequently introduced into U87MG parental cells using previously described methods (Nishikawa et al., 1994). Clones were screened initially by FACS analysis to confirm de2-7EGFR expression. Cells which stained positively for de2-7EGFR were sorted by FACS for high expression and expanded. This population of cells was tested by western blotting for de2-7EGFR expression (mAb806) and loss of phosphorylated Y845 using a phosphorylation-specific antibody against the site.

A *Pme*I fragment containing activated *Src* cDNA (Y529F mutation) was subcloned into the pcDNA3.1/Hygro^{+} vector (Life Technologies) before transfection of the U87MG.Δ2-7 and U87MG.Δ2-7_{845F} cell lines. Transfected cells were screened by FACS to confirm that expression of de2-7EGFR was retained. Clones were then subjected to further analysis by intracellular FACS and western blot using the Src-specific antibody, v-Src 327. Finally, clones showing increased Src expression were western blotted with the phosphorylated-Src-specific antibody, Y418 (Biosource International) to ensure the Src was active. All cell lines were tested by FACS to ensure levels of de2-7EGFR and Src were equal in the different cell lines.

Cell growth and survival at different concentrations of glucose

U87MG and U87MG.Δ2-7 cells were plated at 4×10^4 cells per well in six-well tissue culture plates in 10% fetal bovine serum. On the next day, cells were washed in phosphate-buffered saline, and medium was changed to one containing 10% FBS, glutamine, pyruvate, and glucose at doses of 25, 5, 1, 0.5 and 0 mM. Floating cells were collected and combined with trypsinised plated cells and viable and non-viable cells counted using a hemocytometer on each day.

Isolation and purification of ER

A crude ER sample was isolated from 10^7 exponentially growing U87MG.Δ2-7 cells, using the Endoplasmic Reticulum Isolation Kit (Sigma), as per the manufacturer's instructions. The final ER pellet obtained using this kit was further purified using discontinuous sucrose gradients. Briefly, the ER pellet was resuspended in Buffer A (20 mM HEPES, pH 7.6, 220 mM mannitol, 70 mM sucrose, 1 mM EDTA and 0.5 mM PMSF), before loading the ER sample on top of a discontinuous sucrose density gradient consisting of 15%, 30% and 60% sucrose solutions. The gradient was subjected to ultracentrifugation at 24,000 r.p.m. at 4℃ for 18 hours, using a Beckman Ultracentrifuge fitted with a SW28 rotor. 0.5–1.0 ml fractions were collected from the top of the centrifuge and subsequently tested against a panel of organelle marker antibodies via western blot. Fractions that tested positive against the ER marker antibody calnexin, but negative against all other organelle marker antibodies, were pooled.

Isolation and purification of the mitochondria

6×10^6 exponentially growing cells were harvested, washed twice in ice-cold PBS, and 'crude' mitochondria isolated, in accordance with previously described methods (Johnston et al., 2002; McKenzie et al., 2006). The mitochondrial pellet was stripped of contaminating organelles using a high-salt wash buffer (250 mM sucrose, 1 mM EDTA, 4 M NaCl, 10 mM Tris-HCl, pH 7.4) (Crowley and Payne, 1998; Walter and Blobel, 1983). Following ten high-salt wash steps, the mitochondria were re-isolated by centrifugation at 8000 ***g*** at 4℃ for 15 minutes.

Determination of de2-7EGFR location within the mitochondria

The locality of mitochondria-associated de2-7EGFR was examined biochemically as detailed elsewhere (Gough et al., 2009; Vande Velde et al., 2008), with some modifications. Briefly, samples were halved before proteinase K (PK) digestion (+PK) or a 'sham digest' in Buffer B (500 mM Sucrose, 10 mM HEPES, pH 7.4) (–PK) at 37℃ for 15 minutes. Digestion reactions were stopped by incubating mitochondria with PMSF at 4℃ for 5 minutes. Following two wash steps in Buffer B, mitochondria were re-isolated at 8000 ***g***, 4℃ for 15 minutes and resolved by SDS-PAGE in 2× sample reducing buffer [2.0 ml of Glycerol, 4% (w/v) SDS, 0.005% (w/v) Bromophenol Blue, 0.5 ml of β-mercaptoethanol, 125 mM Tris-HCl, pH 6.8, and ddH_2O].

Preparation of samples and controls for electrophoresis

Whole-cell lysates were prepared by lysis in RIPA buffer (50 mM Tris-HCl, pH 7.5, 150 mM NaCl, 5 mM EDTA, 200 mM Na_3VO_4, 0.5% sodium deoxycholate, 0.05% SDS, 10 mM NaF and protease inhibitor cocktail set 1 from Calbiochem), then sonicated for 15 minutes and centrifuged at 14,000 ***g*** for 30 minutes at 4℃. The supernatant (lysate) was collected and added to equal volumes of 2× sample reducing buffer. Mitochondrial pellets were resuspended in RIPA lysis buffer and sonicated for 15 minutes. Following sonication, equal volumes of 2× sample reducing buffer were added to the sample. All samples were heated at 95℃ for 5 minutes, directly before electrophoresis.

Immunoprecipitation and immunoblot analysis

Cell lysates were immunoprecipitated with relevant antibodies using methods described by us in detail previously (Gan et al., 2007; Johns et al., 2004). Samples were resolved on NuPAGE gels (either 3–8% or 4–12%) as previously described (Gan et al., 2007), followed by the electro-transfer of proteins onto PVDF membranes using the iBlot Gel Transfer System (Life Technologies) as per the manufacturer's instructions. Membranes were blotted with antibodies as detailed in the relevant figure legends, before detection of bands by chemiluminescence radiography using the Storm 804 Phosphorimager (Amersham Biosciences, Piscataway, NJ). Analysis of western blots were performed using ImageQuant TL Image Analysis Software, version 2005 (Gan et al., 2007; Hagar et al., 2003).

Stimulation of SFKs with matrigel

The extracellular matrix gel, matrigel (Sigma) was prepared in serum-free DMEM/F-12 medium (1:50), before application of a thin layer (100 μl) to wells holding sterile 18 mm glass coverslips. Following a 1 hour incubation step at room temperature, excess matrigel was removed and coverslips were subsequently washed twice with serum-free DMEM/F-12 medium. U87MG.Δ2-7 cells (2×10^5 per well) were grown on matrigel-coated coverslips, under normal culture conditions for 24 hours.

Confocal microscopy analysis

Cells grown overnight on 18 mm glass coverslips, were washed twice with PBS, fixed with 4% paraformaldehyde in PBS for 10 minutes, permeabilised with 0.1% Triton X-100 for 10 minutes at room temperature, and subsequently blocked with Image-iT^{TM} FX signal enhancer (Molecular Probes) as per the manufacturer's instructions. The cells were then immunostained for 1 hour at room temperature with primary antibodies, washed twice with 0.1% Triton X-100 in PBS and counterstained with Alexa-Fluor-488- and/or 596-conjugated secondary antibodies (Molecular Probes, 1:2000), for 20 minutes at room temperature. Once washed, coverslips were mounted onto superfrost glass slides over a droplet of mounting media (0.23 g of 1,4-diazabicyclo[2.2.2]octane; Sigma) in 200 μl of ddH_2O and subsequently examined. The mitochondria of viable cells were stained with 500 nM MTR (Molecular Probes) in serum-free medium at 37℃ for 30 minutes, before fixing, permeabilisation and subsequent immunostaining of cells.

Image acquisition

Cells were examined and images acquired using a TCS SP2 confocal laser-scanning microscope (Leica). In all experiments, multiple *z*-section scans (14–16) at 0.15 μm increments spanning the entire depth of the cell were acquired under the same confocal microscope settings (i.e. sequential scans, with wavelengths set as follows: green, 500–535; red, 570–650), using a planApo 100×/1.40 oil immersion, objective lens (Leica). The only exception was where detector gain adjustments were performed to normalise saturation levels in the green channel.

Computational analysis of images

Colocalisation was determined following the voxel analysis of acquired images using a colocalisation macro operated under ImageJ v1.38d software (National Institutes of Health). This plug-in considers two voxels (from the red A, mitochondria and green B, de2-7EGFR channels) as colocalised if their respective intensities are higher than the threshold of their respective channels (default setting: 50 grey levels), and their ratio of intensity is higher than the default ratio setting value of 50% (Gotliv et al., 2006). Following analysis, the program creates a new image where colocalised voxels are highlighted in white. In all cases, computational analysis began with a region of interest (ROI) drawn either around the circumference of the cell in order to determine the percentage of total de2-7EGFR (channel B) expressed by the cell colocalised with mitochondria (channel A), or drawn around the mitochondria in order to determine the percentage of mitochondria within the cell colocalised with de2-7EGFR. Calculations were performed using ImageJ (NIH) and an established formula ($[\Sigma Bi_{\{i\ \varepsilon\ Coloc\}}/\Sigma Ai_{\{i\ \varepsilon\ Mask\}}]3100$), detailed elsewhere (Abramoff et al., 2004).

Electron microscopy analysis

Mitochondria from human glioblastoma cell lines were isolated and purified as detailed above. Once purified, the mitochondrial samples were incubated with 1 μg/ml mAb806, in 1% HSA in PBS (v/v), on ice for 2 hours. Samples were subsequently washed with ice-cold PBS to remove unbound antibody and counterstained on ice for 2 hours with a gold-conjugated secondary antibody

(Sigma) at a 1:500 dilution in Buffer C (0.5 M NaCl, 0.1% BSA, 0.05% Tween20, 5% fetal bovine serum, buffered to pH 7.4). The mitochondrial samples were washed again to remove unbound gold, fixed at room temperature for 10 minutes in 2.4% paraformaldehyde in PBS, washed again and subsequently resuspended in a 1:1 solution consisting of mitochondria storage buffer (Johnston et al., 2002) and agarose. Thereafter, labelled mitochondria were processed and embedded in resin, sectioned and photographed using a JEOL JEM-1200 EX transmission electron microscope.

Measurement of cellular oxygen consumption rate and extracellular acidification rate

U87MG and U87MG.Δ2-7 cells were maintained in DMEM containing 25 mM glucose, 4 mM glutamine and 1 mM pyruvate (Invitrogen, Carlsbad, CA). Oligomycin, carbonyl cyanide p-trifluoromethoxyphenylhydrazone (FCCP) and antimycin were obtained from Sigma, and stock solutions were prepared following the manufacturer's instruction. An extracellular flux (XF) analyzer (Seahorse Bioscience, North Billerica, MA) was used to determine metabolic phenotype of U87MG and U87MG.Δ2-7 cells. XF Analyzer simultaneously monitors oxygen consumption rate (OCR) and extracellular acidification rate (ECAR), which are indicators of mitochondrial respiration and aerobic glycolysis (lactate production), respectively, of cultured cells (Wu et al., 2007). The OCR and ECAR measurements were carried out as described previously (Wu et al., 2007). Briefly, cells were plated at densities of 20,000 cell per well in XF96 cell culture plates and 40,000/well in XF24 cell culture plates, and incubated for 24 hours in 37℃ incubators at 10% CO_2 and 100% humidity. Before measurements, the growth medium was replaced with 600 µl assay medium (Seahorse Bioscience), a low buffered DMEM containing no bicarbonate, and incubated for 45 minutes in a 37℃ non-CO_2 incubator. The concentration of glucose, glutamine and pyruvate concentrations in the assay medium are as indicated in the figure legends. Basal oxygen consumption rate and extracellular acidification rate was determined using XF96 Extracellular Flux analyzer. Mitochondrial function of the cells was assessed using XF24 analyzer. After the measurements, cells were removed from each well with trypsin-EDAT and the number of viable cells was determined using ViCell (Beckman Coulter, CA). The number of cells in each well was used to normalise OCR and ECAR was obtained.

This grant was funded in part by the National Health & Medical Council of Australia (Project Grant 433615 and 1012020) and the James S. McDonnell Foundation (#220020173).

Supplementary material available online at
http://jcs.biologists.org/lookup/suppl/doi:10.1242/jcs.083295/-/DC1

References

Abramoff, M. D., Magelhaes, P. J. and Ram, S. J. (2004). Image processing with ImageJ. *Biophotonics Int.* **11**, 36-42.

Boerner, J. L., Demory, M. L., Silva, C. and Parsons, S. J. (2004). Phosphorylation of Y845 on the epidermal growth factor receptor mediates binding to the mitochondrial protein cytochrome c oxidase subunit II. *Mol. Cell. Biol.* **24**, 7059-7071.

Bonnet, S., Archer, S. L., Allalunis-Turner, J., Haromy, A., Beaulieu, C., Thompson, R., Lee, C. T., Lopaschuk, G. D., Puttagunta, L., Harry, G. et al. (2007). A mitochondria-K+ channel axis is suppressed in cancer and its normalization promotes apoptosis and inhibits cancer growth. *Cancer Cell* **11**, 37-51.

Carpenter, G. and Liao, H. J. (2009). Trafficking of receptor tyrosine kinases to the nucleus. *Exp. Cell Res.* **315**, 1556-1566.

Chakravarti, A., Zhai, G., Suzuki, Y., Sarkesh, S., Black, P. M., Muzikansky, A. and Loeffler, J. S. (2004). The prognostic significance of phosphatidylinositol 3-kinase pathway activation in human gliomas. *J. Clin. Oncol.* **22**, 1926-1933.

Chiu, V. K., Bivona, T., Hach, A., Sajous, J. B., Silletti, J., Wiener, H., Johnson, R. L., 2nd, Cox, A. D. and Philips, M. R. (2002). Ras signalling on the endoplasmic reticulum and the Golgi. *Nat. Cell Biol.* **4**, 343-350.

Clark, E. A. and Brugge, J. S. (1995). Integrins and signal transduction pathways: the road taken. *Science* **268**, 233-239.

Crowley, K. S. and Payne, R. M. (1998). Ribosome binding to mitochondria is regulated by GTP and the transit peptide. *J. Biol. Chem.* **273**, 17278-17285.

de la Iglesia, N., Konopka, G., Puram, S. V., Chan, J. A., Bachoo, R. M., You, M. J., Levy, D. E., Depinho, R. A. and Bonni, A. (2008). Identification of a PTEN-regulated STAT3 brain tumor suppressor pathway. *Genes Dev.* **22**, 449-462.

Demory, M. L., Boerner, J. L., Davidson, R., Faust, W., Miyake, T., Lee, I., Huttemann, M., Douglas, R., Haddad, G. and Parsons, S. J. (2009). Epidermal growth factor receptor translocation to the mitochondria: regulation and effect. *J. Biol. Chem.* **284**, 36592-36604.

Ekstrand, A. J., Sugawa, N., James, C. D. and Collins, V. P. (1992). Amplified and rearranged epidermal growth factor receptor genes in human glioblastomas reveal deletions of sequences encoding portions of the N- and/or C-terminal tails. *Proc. Natl. Acad. Sci. USA* **89**, 4309-4313.

Frederick, L., Wang, X. Y., Eley, G. and James, C. D. (2000). Diversity and frequency of epidermal growth factor receptor mutations in human glioblastomas. *Cancer Res.* **60**, 1383-1387.

Fukai, J., Nishio, K., Itakura, T. and Koizumi, F. (2008). Antitumor activity of cetuximab against malignant glioma cells overexpressing EGFR deletion mutant variant III. *Cancer Sci.* **99**, 2062-2069.

Gan, H. K., Walker, F., Burgess, A. W., Rigopoulos, A., Scott, A. M. and Johns, T. G. (2007). The epidermal growth factor receptor (EGFR) tyrosine kinase inhibitor AG1478 increases the formation of inactive untethered EGFR dimers: implications for combination therapy with monoclonal antibody 806. *J. Biol. Chem.* **282**, 2840-2850.

Goel, S., Hidalgo, M. and Perez-Soler, R. (2007). EGFR inhibitor-mediated apoptosis in solid tumors. *J. Exp. Ther. Oncol.* **6**, 305-320.

Gotliv, B. A., Robach, J. S. and Veis, A. (2006). The composition and structure of bovine peritubular dentin: mapping by time of flight secondary ion mass spectroscopy. *J. Struct. Biol.* **156**, 320-333.

Gough, D. J., Corlett, A., Schlessinger, K., Wegrzyn, J., Larner, A. C. and Levy, D. E. (2009). Mitochondrial STAT3 supports Ras-dependent oncogenic transformation. *Science* **324**, 1713-1716.

Guo, D., Hildebrandt, I. J., Prins, R. M., Soto, H., Mazzotta, M. M., Dang, J., Czernin, J., Shyy, J. Y., Watson, A. D., Phelps, M. et al. (2009). The AMPK agonist AICAR inhibits the growth of EGFRvIII-expressing glioblastomas by inhibiting lipogenesis. *Proc. Natl. Acad. Sci. USA* **106**, 12932-12937.

Hagar, W., Vichinsky, E. P. and Theil, E. C. (2003). Liver ferritin subunit ratios in neonatal hemochromatosis. *Pediatr. Hematol. Oncol.* **20**, 229-235.

Heimberger, A. B., Learn, C. A., Archer, G. E., McLendon, R. E., Chewning, T. A., Tuck, F. L., Pracyk, J. B., Friedman, A. H., Friedman, H. S., Bigner, D. D. et al. (2002). Brain tumors in mice are susceptible to blockade of epidermal growth factor receptor (EGFR) with the oral, specific, EGFR-tyrosine kinase inhibitor ZD1839 (iressa). *Clin. Cancer Res.* **8**, 3496-3502.

Huang, P. H., Mukasa, A., Bonavia, R., Flynn, R. A., Brewer, Z. E., Cavenee, W. K., Furnari, F. B. and White, F. M. (2007). Quantitative analysis of EGFRvIII cellular signaling networks reveals a combinatorial therapeutic strategy for glioblastoma. *Proc. Natl. Acad. Sci. USA* **104**, 12867-12872.

Humphrey, P. A., Gangarosa, L. M., Wong, A. J., Archer, G. E., Lund-Johansen, M., Bjerkvig, R., Laerum, O. D., Friedman, H. S. and Bigner, D. D. (1991). Deletion-mutant epidermal growth factor receptor in human gliomas: effects of type II mutation on receptor function. *Biochem. Biophys. Res. Commun.* **178**, 1413-1420.

Johns, T. G., Stockert, E., Ritter, G., Jungbluth, A. A., Huang, H. J., Cavenee, W. K., Smyth, F. E., Hall, C. M., Watson, N., Nice, E. C. et al. (2002). Novel monoclonal antibody specific for the de2-7 epidermal growth factor receptor (EGFR) that also recognizes the EGFR expressed in cells containing amplification of the EGFR gene. *Int. J. Cancer* **98**, 398-408.

Johns, T. G., Adams, T. E., Cochran, J. R., Hall, N. E., Hoyne, P. A., Olsen, M. J., Kim, Y.-S., Rothacker, J., Nice, E. C., Walker, F. et al. (2004). Identification of the epitope for the epidermal growth factor receptor-specific monoclonal antibody 806 reveals that it preferentially recognizes an untethered form of the receptor. *J. Biol. Chem.* **279**, 30375-30384.

Johns, T. G., Mellman, I., Cartwright, G. A., Ritter, G., Old, L. J., Burgess, A. W. and Scott, A. M. (2005). The antitumor monoclonal antibody 806 recognizes a high-mannose form of the EGF receptor that reaches the cell surface when cells over-express the receptor. *FASEB J.* **19**, 780-782.

Johns, T. G., Perera, R. M., Vernes, S. C., Vitali, A. A., Cao, D. X., Cavenee, W. K., Scott, A. M. and Furnari, F. B. (2007). The efficacy of epidermal growth factor receptor-specific antibodies against glioma xenografts is influenced by receptor levels, activation status, and heterodimerization. *Clin. Cancer Res.* **13**, 1911-1925.

Johnston, A. J., Hoogenraad, J., Dougan, D. A., Truscott, K. N., Yano, M., Mori, M., Hoogenraad, N. J. and Ryan, M. T. (2002). Insertion and assembly of human tom7 into the preprotein translocase complex of the outer mitochondrial membrane. *J. Biol. Chem.* **277**, 42197-42204.

Li, B., Yuan, M., Kim, I. A., Chang, C. M., Bernhard, E. J. and Shu, H. K. (2004). Mutant epidermal growth factor receptor displays increased signaling through the phosphatidylinositol-3 kinase/AKT pathway and promotes radioresistance in cells of astrocytic origin. *Oncogene* **23**, 4594-4602.

Lu, K. V., Zhu, S., Cvrljevic, A., Huang, T. T., Sarkaria, S., Ahkavan, D., Dang, J., Dinca, E. B., Plaisier, S. B., Oderberg, I. et al. (2009). Fyn and SRC are effectors of oncogenic epidermal growth factor receptor signaling in glioblastoma patients. *Cancer Res.* **69**, 6889-6898.

Luwor, R. B., Johns, T. G., Murone, C., Huang, H. J., Cavenee, W. K., Ritter, G., Old, L. J., Burgess, A. W. and Scott, A. M. (2001). Monoclonal antibody 806 inhibits the growth of tumor xenografts expressing either the de2-7 or amplified epidermal growth factor receptor (EGFR) but not wild-type EGFR. *Cancer Res.* **61**, 5355-5361.

Maher, E. A., Furnari, F. B., Bachoo, R. M., Rowitch, D. H., Louis, D. N., Cavenee, W. K. and DePinho, R. A. (2001). Malignant glioma: genetics and biology of a grave matter. *Genes Dev.* **15**, 1311-1333.

McKenzie, M., Lazarou, M., Thorburn, D. R. and Ryan, M. T. (2006). Mitochondrial respiratory chain supercomplexes are destabilized in Barth Syndrome patients. *J. Mol. Biol.* **361**, 462-469.

Mellinghoff, I. K., Wang, M. Y., Vivanco, I., Haas-Kogan, D. A., Zhu, S., Dia, E. Q., Lu, K. V., Yoshimoto, K., Huang, J. H., Chute, D. J. et al. (2005). Molecular determinants of the response of glioblastomas to EGFR kinase inhibitors. *N. Engl. J. Med.* **353**, 2012-2024.

Mizoguchi, M., Betensky, R. A., Batchelor, T. T., Bernay, D. C., Louis, D. N. and Nutt, C. L. (2006). Activation of STAT3, MAPK, and AKT in malignant astrocytic gliomas: correlation with EGFR status, tumor grade, and survival. *J. Neuropathol. Exp. Neurol.* **65**, 1181-1188.

Montgomery, R. B. (2002). Antagonistic and agonistic effects of quinazoline tyrosine kinase inhibitors on mutant EGF receptor function. *Int. J. Cancer* **101**, 111-117.

Moscatello, D. K., Holgado-Madruga, M., Emlet, D. R., Montgomery, R. B. and Wong, A. J. (1998). Constitutive activation of phosphatidylinositol 3-kinase by a naturally occurring mutant epidermal growth factor receptor. *J. Biol. Chem.* **273**, 200-206.

Nagane, M., Coufal, F., Lin, H., Bogler, O., Cavenee, W. K. and Huang, H. J. (1996). A common mutant epidermal growth factor receptor confers enhanced tumorigenicity on human glioblastoma cells by increasing proliferation and reducing apoptosis. *Cancer Res.* **56**, 5079-5086.

Nagane, M., Levitzki, A., Gazit, A., Cavenee, W. K. and Huang, H. J. (1998). Drug resistance of human glioblastoma cells conferred by a tumor-specific mutant epidermal growth factor receptor through modulation of Bcl-XL and caspase-3-like proteases. *Proc. Natl. Acad. Sci. USA* **95**, 5724-5729.

Naresh, A., Long, W., Vidal, G. A., Wimley, W. C., Marrero, L., Sartor, C. I., Tovey, S., Cooke, T. G., Bartlett, J. M. and Jones, F. E. (2006). The ERBB4/HER4 intracellular domain 4ICD is a BH3-only protein promoting apoptosis of breast cancer cells. *Cancer Res.* **66**, 6412-6420.

Narita, Y., Nagane, M., Mishima, K., Huang, H. J., Furnari, F. B. and Cavenee, W. K. (2002). Mutant epidermal growth factor receptor signaling down-regulates p27 through activation of the phosphatidylinositol 3-kinase/Akt pathway in glioblastomas. *Cancer Res.* **62**, 6764-6769.

Nishikawa, R., Ji, X. D., Harmon, R. C., Lazar, C. S., Gill, G. N., Cavenee, W. K. and Huang, H. J. (1994). A mutant epidermal growth factor receptor common in human glioma confers enhanced tumorigenicity. *Proc. Natl. Acad. Sci. USA* **91**, 7727-7731.

Perera, R. M., Narita, Y., Furnari, F. B., Gan, H. K., Murone, C., Ahlkvist, M., Luwor, R. B., Burgess, A. W., Stockert, E., Jungbluth, A. A. et al. (2005). Treatment of human tumor xenografts with monoclonal antibody 806 in combination with a prototypical epidermal growth factor receptor-specific antibody generates enhanced antitumor activity. *Clin. Cancer Res.* **11**, 6390-6399.

Pillay, V., Allaf, L., Wilding, A. L., Donoghue, J. F., Court, N. W., Greenall, S. A., Scott, A. M. and Johns, T. G. (2009). The plasticity of oncogene addiction: implications for targeted therapies directed to receptor tyrosine kinases. *Neoplasia* **11**, 448-58, 2 p following 458.

Schmidt, M. H., Furnari, F. B., Cavenee, W. K. and Bogler, O. (2003). Epidermal growth factor receptor signaling intensity determines intracellular protein interactions, ubiquitination, and internalization. *Proc. Natl. Acad. Sci. USA* **100**, 6505-6510.

Sugawa, N., Ekstrand, A. J., James, C. D. and Collins, V. P. (1990). Identical splicing of aberrant epidermal growth factor receptor transcripts from amplified rearranged genes in human glioblastomas. *Proc. Natl. Acad. Sci. USA* **87**, 8602-8606.

Swinnen, J. V., Brusselmans, K. and Verhoeven, G. (2006). Increased lipogenesis in cancer cells: new players, novel targets. *Curr. Opin. Clin. Nutr. Metab. Care* **9**, 358-365.

Ursini-Siegel, J., Rajput, A. B., Lu, H., Sanguin-Gendreau, V., Zuo, D., Papavasiliou, V., Lavoie, C., Turpin, J., Cianflone, K., Huntsman, D. G. et al. (2007). Elevated expression of DecR1 impairs ErbB2/Neu-induced mammary tumor development. *Mol. Cell. Biol.* **27**, 6361-6371.

Vande Velde, C., Miller, T. M., Cashman, N. R. and Cleveland, D. W. (2008). Selective association of misfolded ALS-linked mutant SOD1 with the cytoplasmic face of mitochondria. *Proc. Natl. Acad. Sci. USA* **105**, 4022-4027.

Vander Heiden, M. G., Cantley, L. C. and Thompson, C. B. (2009). Understanding the Warburg effect: the metabolic requirements of cell proliferation. *Science* **324**, 1029-1033.

Walter, P. and Blobel, G. (1983). Preparation of microsomal membranes for cotranslational protein translocation. *Methods Enzymol.* **96**, 84-93.

Warburg, O. (1956a). On respiratory impairment in cancer cells. *Science* **124**, 269-270.

Warburg, O. (1956b). On the origin of cancer cells. *Science* **123**, 309-314.

Wong, A. J., Ruppert, J. M., Bigner, S. H., Grzeschik, C. H., Humphrey, P. A., Bigner, D. S. and Vogelstein, B. (1992). Structural alterations of the epidermal growth factor receptor gene in human gliomas. *Proc. Natl. Acad. Sci. USA* **89**, 2965-2969.

Wu, M., Neilson, A., Swift, A. L., Moran, R., Tamagnine, J., Parslow, D., Armistead, S., Lemire, K., Orrell, J., Teich, J. et al. (2007). Multiparameter metabolic analysis reveals a close link between attenuated mitochondrial bioenergetic function and enhanced glycolysis dependency in human tumor cells. *Am. J. Physiol. Cell Physiol.* **292**, C125-C136.

Yamazaki, H., Ohba, Y., Tamaoki, N. and Shibuya, M. (1990). A deletion mutation within the ligand binding domain is responsible for activation of epidermal growth factor receptor gene in human brain tumors. *Jpn. J. Cancer Res.* **81**, 773-779.